Chemical Engineering Journal 99 (2004) 227–236

Chemical Engineering Journal

www.elsevier.com/locate/cej

Gas phase oxidation of benzoic acid to phenol over nickel oxide catalysts

V. Duma [a], K.E. Popp [a], M.C. Kung [a], H. Zhou [b], S. Nguyen [b], S. Ohyama [c,1], H.H. Kung [a,*], C.L. Marshall [d]

[a] *Department of Chemical Engineering, Northwestern University, 2145 Sheridan Road, Evanston, IL 60201-3120, USA*
[b] *Department of Chemistry, Northwestern University, 2145 Sheridan Road, Evanston, IL 60201-3120, USA*
[c] *Central Research Institute of Electric Power Industry, Tokyo, Japan*
[d] *Chemical Engineering Division, Argonne National Laboratory, Argonne, IL, USA*

Received 5 June 2003; accepted 14 November 2003

Abstract

The catalytic conversion of benzoic acid to phenol in the presence of water and oxygen was studied in the vapor phase over nickel oxide on various supports. NiO/SiO_2 was the most selective, and the selectivity reached over 50% using iron oxide and sodium oxide modifiers. Ni–Fe oxide prepared by coprecipitation deactivated with time-on-stream, but that prepared using a cellulose templating method was more stable. Benzene was often a significant by-product. Some coupling products were formed, including xanthone, fluorenone, and biphenyl. From deuterium isotope labeling experiments, the hydroxyl group was found to be formed at the carbon next to the one with the carboxylic acid group.

Keywords: Benzoic acid; Phenol synthesis; Nickel oxide; Heterogeneous catalysis

1. Introduction

Phenol is a large-scale chemical commodity, with an annual production of more than 5.5 million tonnes [1]. It is used in the production of phenolic and epoxy resins, polycarbonates, nylon, and others. Most of the phenol (>95%) is made by the cumene process [2]. Cumene, formed by alkylation of benzene with propene, is oxidized with air to form cumene hydroperoxide, which is cleaved in the presence of a liquid acid catalyst to yield phenol and acetone. Thus, the economics of phenol production by this process is influenced by the demand for acetone.

A second, minor route for the production of phenol is the toluene–benzoic acid process. Toluene is oxidized in the presence of air and a cobalt salt catalyst to benzoic acid. Then, the benzoic acid is oxidized with air and a catalyst mixture of copper and magnesium salts to phenyl benzoate, which is then hydrolyzed to yield phenol.

Both of these processes are performed in the liquid phase and produce large amounts of liquid waste. From both economic and environmental points of view, the synthesis of phenol by a more direct gas phase oxidation process is highly desirable. Despite many attempts, no gas phase process for the direct oxidation of benzene with oxygen to phenol has been developed. On the other hand, there were indications in the literature that showed promise for a gas phase process by oxidation of toluene.

The oxidation of toluene to benzoic acid can be performed in the vapor phase over vanadia catalysts [3–5]. For the gas phase oxidation of benzoic acid to phenol, two types of catalysts were reported in the literature: copper oxide catalysts and, more recently, nickel oxide catalysts. Stolkova and coworkers [6–8] studied a variety of copper oxide catalysts and reported selectivity to phenol of 84% at a benzoic acid conversion of 33 and 52% over the supported catalysts $Cu–Bi–Cd/Al_2O_3$ and $Cu–Bi–Pb/Al_2O_3$, respectively. Miki et al. [9–17] claimed better results for their nickel oxide-based catalysts. They reported selectivities to phenol higher than 90% at a benzoic acid conversion of 100% for the nickel–iron oxide coprecipitated catalysts [14,15]. However, the selectivity was reported to depend on the calcination temperature sensitively, and the high selectivity was obtained only for 800 °C calcination. In these experiments, the reaction mixture (benzoic acid, air, water and nitrogen)

* Corresponding author.
E-mail address: hkung@northwestern.edu (H.H. Kung).
[1] On leave.

1385-8947/$ – see front matter © 2003 Elsevier B.V. All rights reserved.
doi:10.1016/j.cej.2003.11.012

was fed continuously into a fused silica reactor containing the catalyst. The products were collected at the reactor outlet by a cooling trap filled with acetone at 0 °C and a second one with methanol and dry ice and analyzed offline [15,17].

In view of the rather unusual dependence on calcination temperature reported, we thought it useful to study the role of the individual components in the $NiO–Fe_2O_3$ catalysts and the reaction mechanism. Previously [18], we reported that addition of small amounts of vanadium modifier to a precipitated nickel oxide catalyst improved and stabilized the catalytic activity, whereas vanadium oxide alone predominantly promoted the combustion of benzoic acid to yield carbon oxides.

2. Experimental

2.1. Catalyst preparation and characterization

Precipitated and coprecipitated catalysts were prepared after Miki et al. [9,17]. Aqueous solutions of the precursors (metal nitrates) and sodium hydroxide were added dropwise simultaneously to deionized water while maintaining the pH at 7–8. After stirring at room temperature for 2 h, the resulting precipitate was separated by centrifugation and washed a few times with deionized water. The precipitate was dried at 110 °C and calcined in air at 500–900 °C for 4 h.

Cellulose templated catalysts were prepared after the method described by Shigapov et al. [19]. In this procedure, a series of mixed oxides with different ratios of nickel to iron were prepared by adding a solution of the nickel and iron nitrates to a collection of Whatman 50 filter papers. The moist paper was placed into a furnace at 600 °C for rapid heating, and was kept at 600 °C for 1 h to remove the paper. The resulting solid was calcined at 700 °C for 3 h.

Supported catalysts were prepared by incipient wetness impregnation of the supports with an aqueous solution of the precursor, followed by drying at 110 °C and calcination in air at 500–600 °C for 3 h. A silica gel support was prepared after Shoup [20]. For this, potassium silicate (Kasil 1) was mixed with colloidal silica (Ludox). Formamide was added while stirring, then the solution was allowed to gel. The mass ratio of the components was Kasil1:Ludox:formamide = 8:2:1. The solid gel was leached in dilute aq. HNO_3 to remove residual K. Three different batches were prepared, denoted as S1, S2 and S3 with different extents of leaching. The samples S1 and S2 were leached in a 0.01 vol.% aq. HNO_3 and the S3 sample was leached in a 1 vol.% aq. HNO_3. The preparation of gamma-alumina (γ-Al_2O_3) is described in [21]. Other supports were commercially available materials. A fumed silica gel with the trade name Aerocat from Degussa was denoted hereafter as SiO_2(A). The anatase form of titanium dioxide, from Sachtleben, was denoted as TiO_2(A). Alfa-alumina (α-Al_2O_3), −100 mesh, 99%; yttria stabilized zirconia (ZrO_2), 99.5%, and vanadia (V_2O_5), 99.6%, all from Aldrich, were used as well. Addition of sodium to the catalysts was achieved by impregnation of the catalyst with a 0.01 mol/l aqueous solution of sodium citrate, followed by washing and calcination at 500 °C for 3 h.

The chemicals used include: nickel(II) nitrate hexahydrate, crystal (Aldrich); iron nitrate nonahydrate, >98% (Aldrich); sodium hydroxide, cert. ACS (Fisher Scientific); potassium silicate, Kasil 1 (PQ Corporation); colloidal silica, Ludox (Aldrich); formamide, >99.5% (Aldrich); sodium citrate dihydrate, crystal (Baker).

The catalysts were characterized by surface area measurements, X-ray powder diffraction (XRD), and scanning electron microscopy/energy-dispersive X-ray spectrometry (SEM/EDAX). The BET surface area measurements were conducted by nitrogen adsorption on an Omnisorp 360 automatic system (Omicron Technology) and an ASAP 2010 (Micromeritics). The XRD spectra were collected on a Rigaku diffractometer (Geigerflex) with a Cu Kα radiation source at 40 kV and 20 mA. The SEM/EDAX spectra were recorded on a Hitachi 3500N.

2.2. Reaction experiments

The experiments were conducted in a fixed bed fused silica reactor. The tubular reactor, placed vertically inside the heating furnace, was about 30 cm long and had an i.d. of 1 cm. The reaction mixture consisted of benzoic acid, oxygen, water and helium. Methane was used as an internal standard. Benzoic acid and water were supplied in the gas phase by passing the carrier gas through heated saturators containing these two substances. The product stream was analyzed on-line using a gas chromatograph and mass spectrometer (Hewlett-Packard 6890 GC/5973 MS). The gas chromatograph was equipped with a TCD using a packed column (1.8 m × 1/8 in., Carbosphere 80–100 mesh, Alltech) and a FID using a capillary column (Hewlett Packard, InnoWax polyethylene glycol, 30 m × 0.25 mm × 0.25 μm). Prior to the reaction, the feed by-passed the reactor and was sent to analysis. The conversions of benzoic acid and oxygen and the selectivities to organic products were calculated as follows:

$$X = \frac{A_\mathrm{i} - A_\mathrm{e}}{A_\mathrm{i}}, \tag{1}$$

where X is the conversion, A the peak area, i the inlet, and e is the exit.

$$S_k = \frac{A_{k,\mathrm{e}} f_k}{(A_{\mathrm{BA,i}} - A_{\mathrm{BA,e}}) f_{\mathrm{BA}}}, \tag{2}$$

where S is the selectivity, f the GC sensitivity factor [22], $k$the reaction product, and BA is the benzoic acid.

Since the oxidation of 1 mol of benzoic acid to 1 mol of phenol produces 1 mol of CO_2, this amount of CO_2 was excluded from the calculation of CO_2 selectivity. Likewise, the CO_2 produced in the formation of benzene and coupling products (e.g. biphenyl, xanthone, fluorenone) was excluded. The yield, Y_k to products were calculated as

$$Y_k = X_{\mathrm{BA}} S_k.$$

In a typical experiment, a combined stream of O_2 in He (Matheson, certified grade) and CH_4 in He (Matheson, certified grade) was passed through a heated water saturator at 80 °C. The mixture was then combined with a He stream (Airgas, high purity) carrying benzoic acid (99.5%, Aldrich) from a saturator heated at 145 °C to produce a reaction feed containing ca. 1 mol% benzoic acid, 3% oxygen, 25% water, 0.15% methane and helium. The mixture was sent directly to the GC–MS for analysis or was passed through a heated catalyst bed (≈0.5 g catalyst) at the desired temperature. Carbon balance was typically 95 ± 5%, and there was observable carbonaceous deposits on the catalysts after reaction.

For NMR analysis of the phenol product, the exit stream from the reactor was passed through a trap at 0 °C, and phenol was extracted with CH_2Cl_2. The extracted solution was dried over Na_2SO_4, filtered, and concentrated under reduced pressure to give a blackish product. The phenol recovered was obtained after column chromatography (SiO_2 gel, hexane/ethyl acetate 5:1), and found to show ^{1}H NMR resonances at ($CDCl_3$) δ 7.26 (m, aromatic-4,5-C*H*, 2H), δ 6.94 (m, aromatic-3-C*H*, 1H), δ 6.86 (d, aromatic-6-C*H*, J = 6.1 Hz, 1H), 5.49 (s, O*H*, 1H).

The ^{1}H NMR spectra were recorded on either a Varian Mercury 400 (400 MHz) or Varian Inova 500 (500 MHz) spectrometer. Theoretical ^{1}H NMR spectra were calculated using the computer program ACD Labs, version 4.02 (1999) from Advanced Chemistry Development Inc.

The deuterated benzoic acid was prepared after [23]. First, 4-D-toluene was prepared. For this, a Grignard reagent prepared from 34.2 g (0.2 mol) *para*-bromotoluene and 5.0 g (0.20 mol) magnesium turnings in 150 ml of anhydrous diethyl ether was decomposed with 15 g (0.25 mol) of deuteroacetic acid obtained by hydrolysis of redistilled acetic anhydride with the calculated amount of deuterium oxide. Water was added to dissolve the magnesium salts and the ethereal layer separated. The ethereal solution was washed with sodium hydroxide to remove excess acetic acid, dried over magnesium sulfate, and distilled. The yield of 4-D-toluene was 6.0 g (32%). ^{1}H NMR ($CDCl_3$): δ 7.29 (d, aromatic-2,6-C*H*, J = 6.0 Hz, 2H), δ 7.21 (d, aromatic-3,5-C*H*, J = 7.5 Hz, 2H), δ 2.39 (s, CH_3, 3H). Next, the obtained 4-D-toluene was used to prepare 4-D-benzoic. In this procedure, a mixture of 5.87 g (0.063 mol) 4-D-toluene, 23 g (0.144 mol) potassium permanganate, 1.4 ml 10% aqueous sodium hydroxide, and 250 ml of water was stirred vigorously and gradually heated to reflux. After 11 h, all of the permanganate and 4-D-toluene appeared to be completely reacted as monitored by TLC. The mixture was filtered hot and the manganese dioxide washed with several portions of hot water. The filtrate was concentrated to 130 ml and decolorized with charcoal. The solution was slowly acidified with concentrated hydrochloric acid to pH 3, and the resulting precipitate of benzoic acid was vacuum filtered and dried. Six grams (77%) of 4-D-benzoic acid was obtained as white solid. ^{1}H NMR ($CDCl_3$): δ 8.15 (d, aromatic-2,6-C*H*, J = 7.3 Hz, 2H), δ 7.50 (d, aromatic-3,5-C*H*, J = 7.3 Hz, 2H). A batch of 3-D-phenol was synthesized after [24] to serve as reference to be compared with the phenol prepared by the gas phase oxidation of benzoic acid. For this, a 100 ml Schlenk flask fitted with reflux condenser and a magnetic stir-bar was dried overnight. Two grams 3-bromophenol (0.0115 mol) was added to the dry glassware and dissolved in 25 ml dry ether. This was followed by 14 ml of the solution of *tert*-butyl lithium (1.7 M in hexanes, 0.023 mol) added over 5 min. After heating at 35 °C for 12 h, 1.25 g of D_2O was added while cooling the flask. After 15 min of stirring, the phenol formed was extracted from the ether with 25 ml 1N NaOH. This was followed by acidifying the aqueous extract to pH 5 using 2N HCl, and the phenol was extracted with ether (3 ml × 15 ml). The ether extract was dried over $CaCl_2$, the ether was removed, and the phenol was recovered by distillation under vacuum to yield 0.43 g 3-D-phenol (40%). ^{1}H NMR (CD_2Cl_2) δ 7.26 (m, aromatic-4,5-C*H*, 2H), δ 6.95 (m, aromatic-3-C*H*, 1H), δ 6.85 (d, aromatic-6-C*H*, J = 7.3 Hz, 1H), 5.08 (s, O*H*, 1H).

3. Results

3.1. Physical properties

The surface areas and average pore diameters for some of the supports and catalysts used are listed in Table 1.

The structures of the coprecipitated and cellulose-templated catalysts (calcined at 700 °C for 3 h) with atomic ratio Ni/Fe = 1/1 were examined with XRD and SEM. NiO and $NiFe_2O_4$ were identified by XRD in both preparations (Fig. 1). However, the peaks for the coprecipitated sample were broader, suggesting that the sample possibly had smaller crystalline domains. The SEM micrographs are shown in Fig. 2. The templated sample was much more porous.

Table 1
Surface area and porosity

Support or catalyst	BET surface area (m^2/g)	Average pore diameter (Å)
Silica gel, SiO_2(S1)	24	79
15% NiO/SiO_2(S1)	17	102
15% NiO–15% Fe_2O_3/SiO_2(S1)	15	123
Na/15% NiO–15% Fe_2O_3/SiO_2(S1)	28	124
Silica gel, SiO_2(S2)	21	61
30% NiO/SiO_2(S2)	16	79
Fumed silica gel, SiO_2(A)	614	181
10% NiO/SiO_2(A)	370	185
15% NiO/SiO_2(A)	284	179
15% Co_3O_4/SiO_2(S1)	8	71
5% Co_3O_4/TiO_2	46	147
15% MnO_2/TiO_2	13	123
15% NiO/ZrO_2	8	125
30% NiO/α-Al_2O_3	10	170

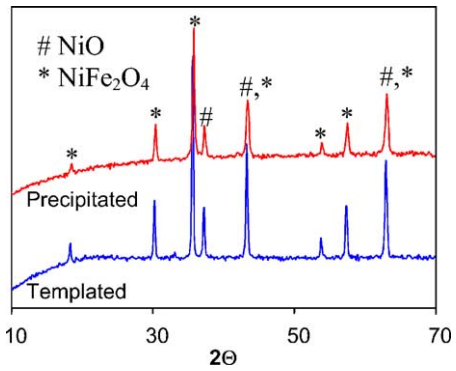

Fig. 1. XRD spectra of a coprecipitated (top) and a templated (bottom) nickel–iron oxide catalyst (atomic ratio Ni/Fe = 1/1).

XRD patterns of the NiO/SiO_2 catalysts all showed detectable NiO peaks. The morphology of the SiO_2 support, however, differed depending on the degree of leaching. This is shown in Fig. 3. The sample that was leached more extensively (S3) showed a rougher surface than S1, whereas the commercial fumed silica had a much smoother surface.

3.2. Effect of calcination temperature on the coprecipitated $NiO–Fe_2O_3$ catalysts

Table 2 shows the results for three coprecipitated nickel–iron oxide catalysts (Ni/Fe = 1/1) that were calcined at different temperatures. The increase in calcination temperature led to a decrease of the surface area and benzoic acid conversion. The catalyst calcined at 900 °C was inferior to the other catalysts. It had lower areal activity, and, even at a much lower conversion, about the same selectivity for phenol as the others.

3.3. Catalyst stability of $NiO–Fe_2O_3$ catalysts

For the coprecipitated $NiO–Fe_2O_3$ catalysts, the conversion of benzoic acid and the selectivity, and consequently the yield to phenol declined with time-on-stream (TOS). Fig. 4 shows the data for a Ni/Fe = 1 sample calcined at 700 °C. The deactivation of the catalysts with TOS is reversible. Treating the catalyst with oxygen at high temperature recovered the lost activity, and carbon oxides were evolved during regeneration. On the other hand, the activity of a sample prepared by the cellulose templated method was much more stable, declining much more slowly with TOS (Fig. 5). The selectivity for phenol remained rather stable also. However, the activity of the templated catalyst was lower, mostly due to its lower surface area of 6 m^2/g, compared with 20.6 m^2/g for the coprecipitated sample.

Table 2
Effect of calcination temperature on coprecipitated $NiO–Fe_2O_3$ (Ni/Fe = 1/1) catalysts

Calcination temperature (°C)	BET surface area (m^2/g)	Conversion (%)	Selectivity (%)		
			Phenol	CO_x	Benzene
700	20.6	75	52	44	3
800	7.4	68	50	46	2
900	3.0	11	51	34	12

Reaction conditions: temperature = 400 °C; space velocity = 10 000 h^{-1} (6.21 g^{-1} h^{-1}); TOS ≈ 10 min.

3.4. Effect of support for NiO catalysts

The activities of NiO supported on α-Al_2O_3, γ-Al_2O_3, ZrO_2, TiO_2, and SiO_2 were compared. The results are shown in Fig. 6. When tested under the same conditions, the catalysts supported on α-Al_2O_3 and TiO_2 showed the highest activity. At the same conversion (by interpolation), silica-supported catalysts showed the highest selectivity, whereas the alumina-supported samples showed poor selectivity. The nature of the other products also differed substantially. The product distributions at 400 °C are shown in Fig. 7. Benzene was the main product over the γ-Al_2O_3-supported catalyst. On the silica-supported sample, there were substantial amounts of xanthone, which is a coupling product.

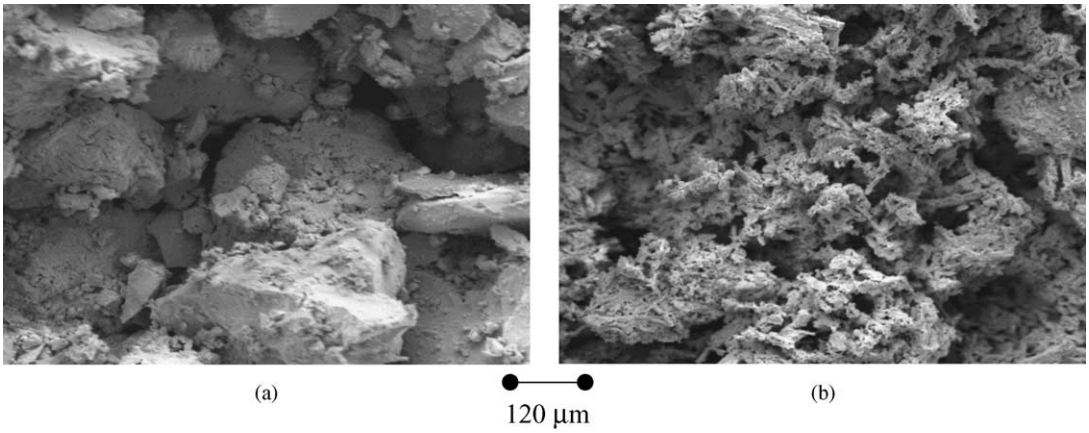

Fig. 2. SEM spectra of a coprecipitated (a) and a templated (b) nickel–iron oxide catalyst (atomic ratio Ni/Fe = 1/1).

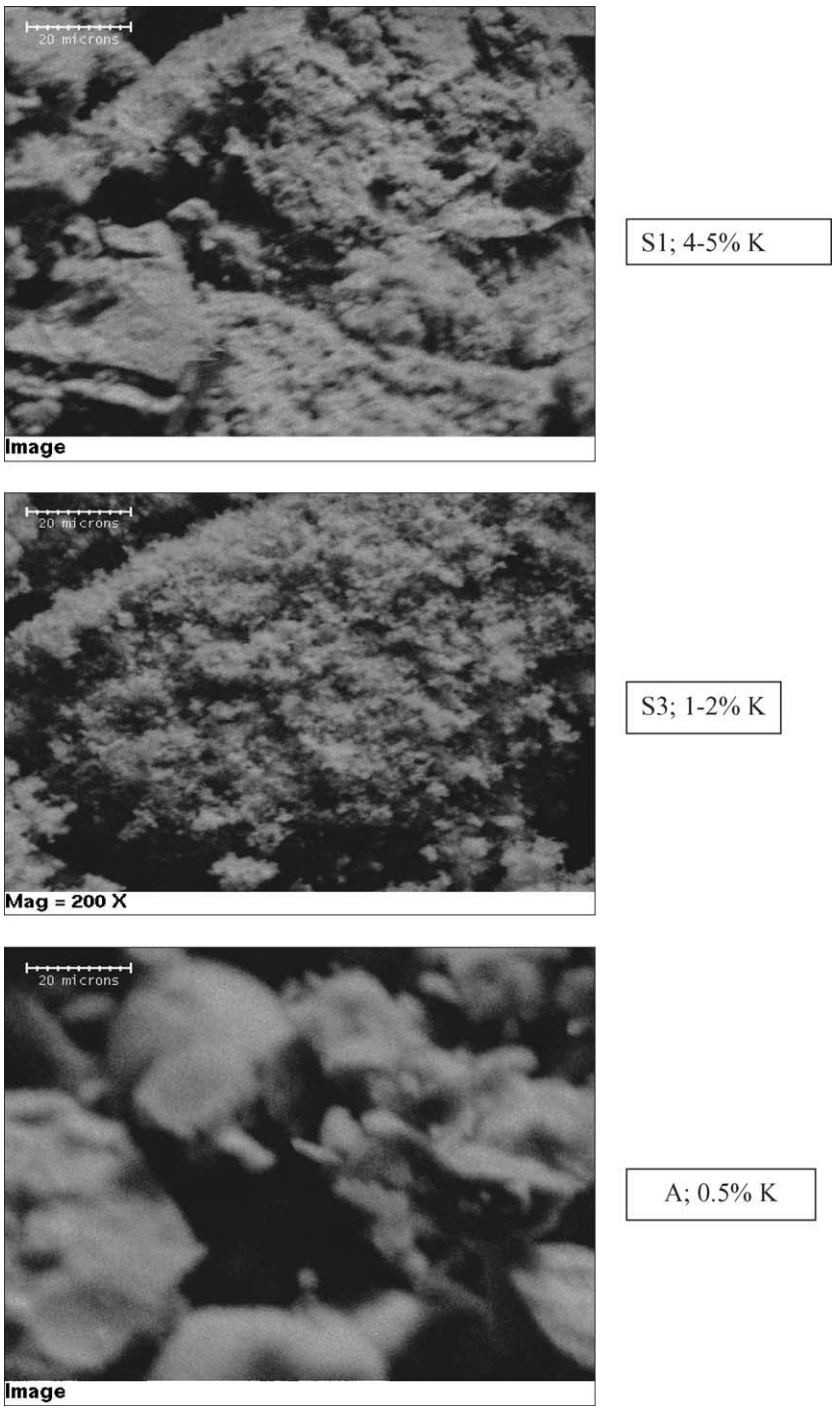

Fig. 3. SEM spectra of silica gel supports. S1, S3—made by gelation from silica sol and potassium silicate; A—commercial fumed silica. Scale bar is 20 μm.

In view of the low combustion selectivity for the silica-supported sample, other silica prepared from the same silica sol but leached to different extents with acid were examined as support. The K contents of these SiO_2 samples were ca. 4–5% for S1 and S2 (same acid leaching, just different batches) and ca. 1–2% for S3. The silica without NiO was already active (Fig. 8). Between these two samples, the silica gel with less K (less basic) (S3) had a slightly higher activity but made a larger amount of coupling products (mainly xanthone).

3.5. Effect of Na and Fe additives

The effects of sodium and iron additives were examined. On NiO/α-Al_2O_3, addition of Na by ion exchange marginally increased its activity (Fig. 9), whereas on

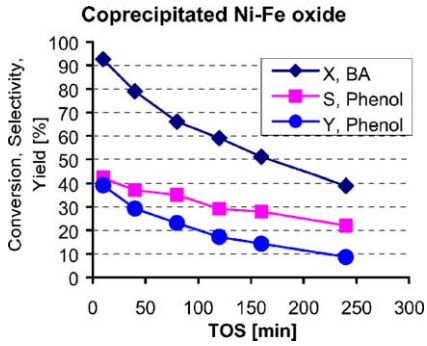

Fig. 4. Benzoic acid oxidation over a coprecipitated nickel–iron oxide catalyst calcined at 700 °C (atomic ratio Ni/Fe = 1/1). Reaction parameters: $T = 400\,^{\circ}C$; SV = 5 l g^{-1} h^{-1}. Feed composition: 1% benzoic acid (BA), 3% O_2, 24% H_2O, balance He. X = conversion of benzoic acid; S, Y = selectivity and yield for phenol, respectively.

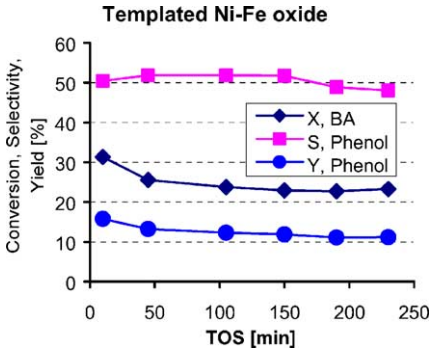

Fig. 5. Benzoic acid oxidation over a templated nickel–iron oxide catalyst calcined at 700 °C (atomic ratio Ni/Fe = 1/1). Reaction parameters: $T = 400\,^{\circ}C$; SV = 5 l g^{-1} h^{-1}. Feed composition: 1% BA, 3% O_2, 24% H_2O, balance He. X = conversion of benzoic acid; S, Y = selectivity and yield for phenol, respectively.

NiO/SiO_2(A) the increase was very large, taking into account the different space velocities (Fig. 10). It also increased the selectivities for phenol and benzene. Addition of Fe (by coprecipitation of the Ni and Fe precursors) to this catalyst also increased its activity and selectivity for phenol (Figs. 9 and 10). On the other hand, addition of both

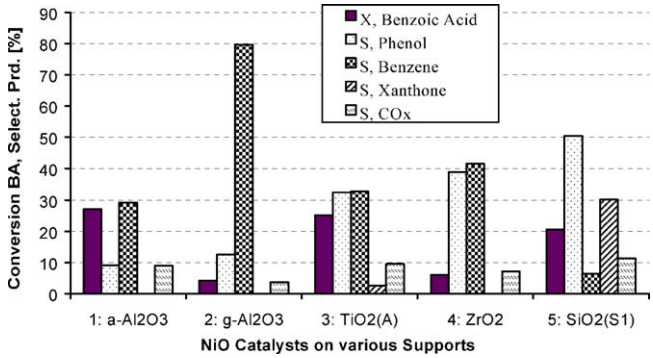

Fig. 7. Benzoic acid conversion (X) and product selectivity (S) over supported nickel oxide catalysts. Catalysts: (1) 30% NiO/α-Al_2O_3; (2) 10% NiO/γ-Al_2O_3; (3) 15% NiO/TiO_2; (4) 15% NiO/ZrO_2; (5) 16% NiO/SiO_2(S1). Reaction parameters: $T = 400\,^{\circ}C$; SV = 5.5–6 l g^{-1} h^{-1}; TOS ≈ 150 min. Feed composition: 1% BA, 3% (1, 2, 3, 4) or 5% (5, 6) O_2, 24% H_2O, balance He.

Fe and Na decreased its activity slightly but increased the phenol selectivity substantially (Fig. 9).

A catalyst containing nickel oxide, iron oxide and sodium supported on silica gel achieved about 40% selectivity to phenol at 50–60% benzoic acid conversion, corresponding to about 20–25% yield to phenol (Fig. 10). The catalyst showed good stability with time on stream. It is possible to attain higher selectivities to phenol at lower conversions, but the yield would be lower (Fig. 11). On this catalyst, significant amounts of coupling products, mainly xanthone, fluorenone and biphenyl were also produced. It was apparent that the amount of xanthrone increased with increasing TOS, suggesting that it was formed from surface species that were accumulated on the surface.

3.6. Effect of water

The effect of water in the feed was examined (Fig. 12). The catalyst deactivated more rapidly in the absence of water. At the same time, the selectivities for both phenol and benzene were suppressed. Removal of oxygen

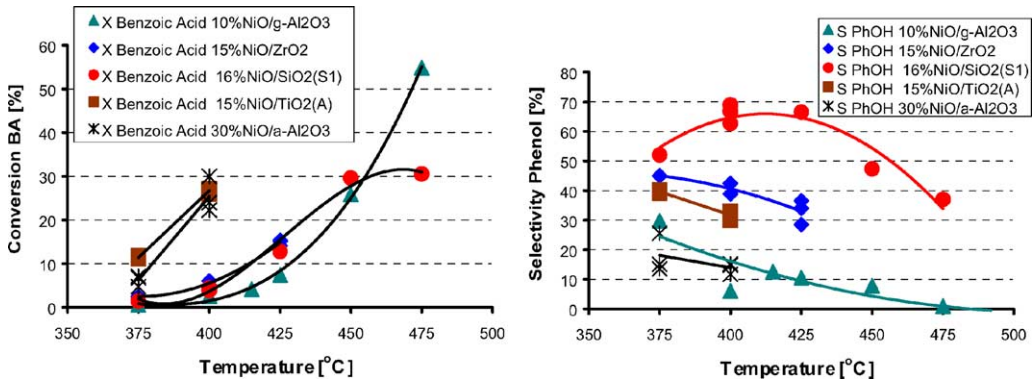

Fig. 6. Benzoic acid conversion (a) and phenol selectivity (b) over supported nickel oxide catalysts vs. temperature. Reaction parameters: T = variable; SV = 5.5–6 l g^{-1} h^{-1}; TOS ≈ 100–150 min. Feed composition: 1% BA, 3% O_2, 25% H_2O, balance He.

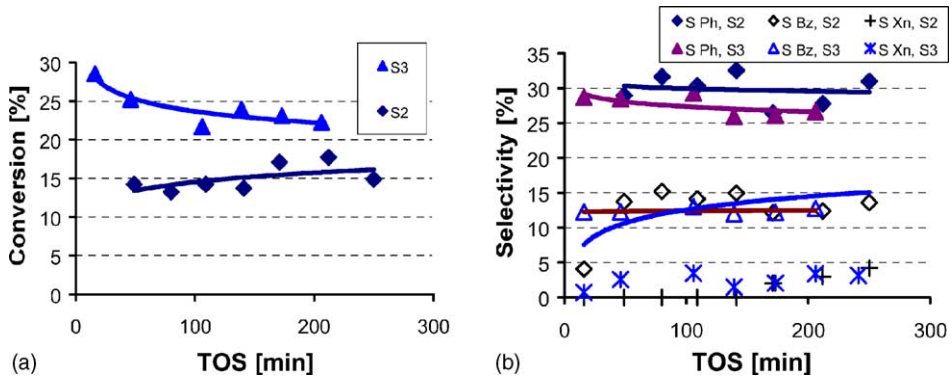

Fig. 8. Benzoic acid conversion (a) and product selectivity (b) (Ph—phenol, Bz—benzene, Xn—xanthone) over silica gels samples S2 and S3 vs. TOS. Reaction parameters: $T = 350\,^{\circ}C$; SV = $5.5\,l\,g^{-1}\,h^{-1}$. Feed composition: 1% BA, 3% O_2, 25% H_2O, balance He.

from the feed resulted in immediate decrease in the conversion.

3.7. Activity of other oxides than NiO

A number of other catalysts were examined briefly for this reaction, and the results are shown in Fig. 12. Compared with NiO catalysts, cobalt oxide, manganese oxide, or vanadium oxide were inferior, showing poorer selectivities to phenol (Figs. 13 and 14).

3.8. Oxidation of para-D-benzoic acid

For the oxidation of deuterated benzoic acid, a 10% NiO/SiO_2(A) catalyst was used. The reactions conditions were: temperature 425 °C, feed composition 1% benzoic acid, 3% oxygen, 25% water, and balance helium. The oxidation of deuterated benzoic acid (4-D-benzoic acid) led to formation of deuterated phenol. The ^1H NMR spectrum of the phenol product (Fig. 15) compared extremely well with

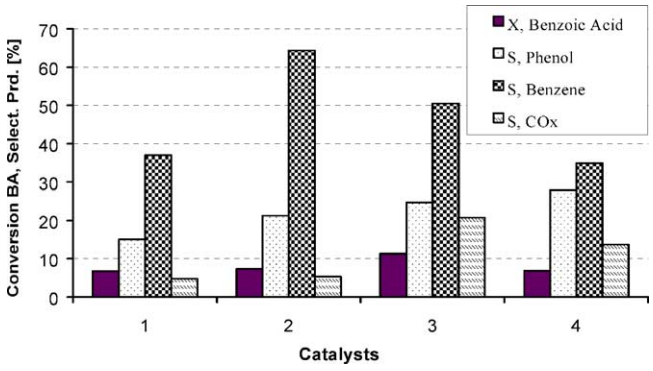

Fig. 9. Effect of Na and Fe additive on benzoic acid conversion and product selectivity over α-alumina supported nickel oxide catalysts. Catalysts: (1) 30% $NiO/\alpha\text{-}Al_2O_3$; (2) Na/30% $NiO/\alpha\text{-}Al_2O_3$; (3) 30% NiO–10% $Fe_2O_3/\alpha\text{-}Al_2O_3$; (4) Na/30% NiO–10% $Fe_2O_3/\alpha\text{-}Al_2O_3$. Reaction parameters: $T = 375\,^{\circ}C$; SV = $5.5\,l\,g^{-1}\,h^{-1}$ (1, 2) or $11\,l\,g^{-1}\,h^{-1}$ (3, 4); TOS ≈ 100 min. Feed composition: 1% BA, 3% O_2, 24% H_2O, balance He. X = conversion of benzoic acid; S = selectivity.

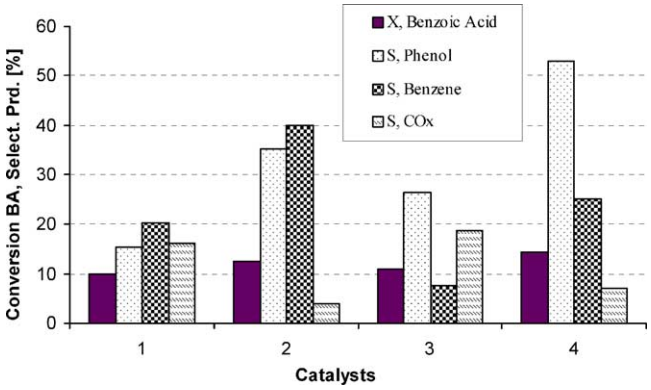

Fig. 10. Benzoic acid conversion and product selectivity over silica supported nickel oxide catalysts. Catalysts: (1) 15% NiO/SiO_2(A); (2) Na/15% NiO/SiO_2(A); (3) 15% NiO–5% Fe_2O_3/SiO_2(A); (4) 16% NiO/SiO_2(S1). Reaction parameters: $T = 375\,^{\circ}C$; SV = $5.5\,l\,g^{-1}\,h^{-1}$ (1, 3), $17\,l\,g^{-1}\,h^{-1}$ (2) or $28.5\,l\,g^{-1}\,h^{-1}$ (4); TOS ≈ 100 min. Feed composition: 1% BA, 3% O_2, 24% H_2O, balance He. X = conversion of benzoic acid; S = selectivity.

the reference 3-D-phenol, as well as with the theoretical spectra of the same compound.

4. Discussion

The development of a heterogeneous catalyst for the oxidation of benzoic acid to phenol would represent an important step toward a process for the gas phase synthesis of phenol from toluene. Although Miki et al. reported high selectivity and activity for coprecipitated nickel–iron oxide catalysts [10–17], unfortunately, in spite of the many attempts we made, the catalysts in this study deactivated rapidly with time-on-stream and showed much lower selectivities (Fig. 4).

The catalysts prepared by the templating technique showed much better stability than the precipitated ones, even though their activities were lower (Fig. 5). The detectable crystalline phases were identical for the two types of catalysts. We postulate that the difference in performance was

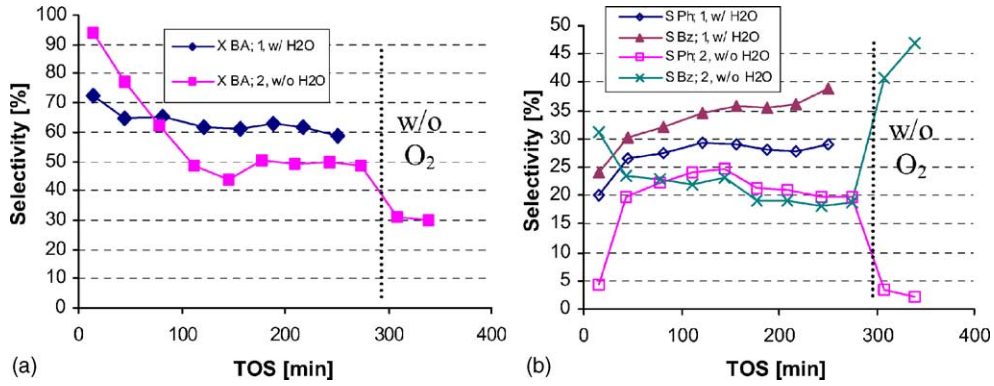

Fig. 11. Benzoic acid conversion (a) and product selectivity (b) (Ph—phenol, Bz—benzene) over the 30% NiO/SiO_2(S2) supported nickel oxide catalyst vs. TOS. Feed composition: (1) 1% BA, 3% O_2, 25% H_2O, balance He; SV = 5.5 l g^{-1} h^{-1}; (2) 1.5% BA, 3.9% O_2, balance He; SV = 4.1 l g^{-1} h^{-1}. Reaction temperature: $T = 400\,^{\circ}C$.

due to their different physical structures. Although the morphology of the templated catalysts was much more spongy (Fig. 2), their surface areas were lower. This suggested that there were very few micropores in these catalysts, making them less susceptible to deactivation by pore blocking.

On many catalysts tested, benzene was the dominant product, which is formed by decarboxylation of benzoic acid. It was formed with a much higher selectivity on alumina-supported catalysts, suggesting that its formation is facilitated by Lewis acid sites. On 16% NiO/SiO_2(S1) and Na/15% NiO–15% Fe_2O_3/SiO_2(S1), however, phenol was the major product. The selectivity for phenol reached over 50% at low benzoic acid conversions, but declined at high conversions. The phenol selectivity depended on the support (Fig. 7), with silica being the best. The results suggest that neutral or basic support is better than acidic support. This is because in this reaction, carbonaceous species on the surface contribute to form coupling products and deactivation. An acidic support facilitates these processes (as well as formation of benzene) and, as a consequence, yields lower selectivity for phenol.

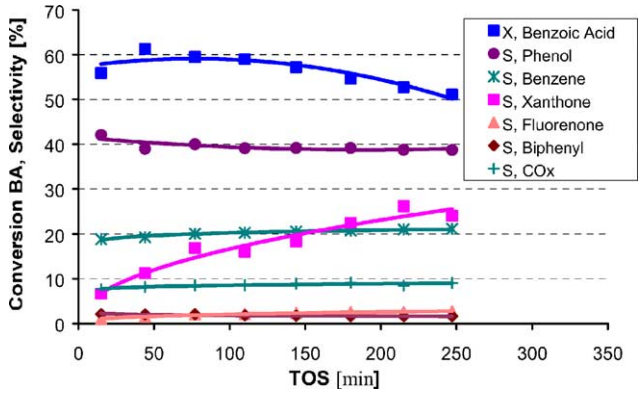

Fig. 12. Benzoic acid conversion (X) and product selectivity (S) over the Na/15% NiO–15% Fe_2O_3/SiO_2(S1) catalyst vs. TOS. Reaction parameters: $T = 375\,^{\circ}C$; SV = 5.5 l g^{-1} h^{-1}. Feed composition: 1% BA, 3% O_2, 25% H_2O, balance He.

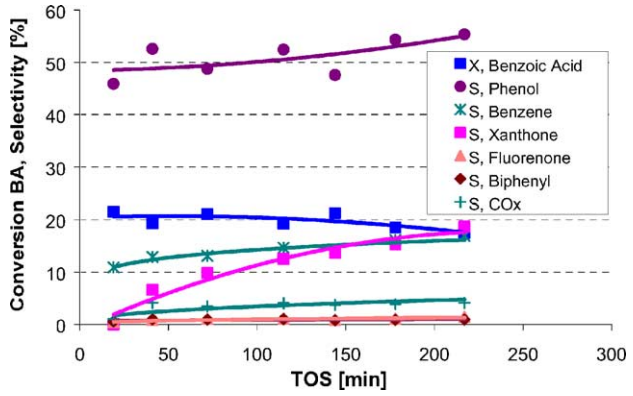

Fig. 13. Benzoic acid conversion (X) and product selectivity (S) over the Na/15% NiO–15% Fe_2O_3/SiO_2(S1) catalyst vs. TOS. Reaction parameters: $T = 350\,^{\circ}C$; SV = 5.5 l g^{-1} h^{-1}. Feed composition: 1% BA, 3% O_2, 25% H_2O, balance He.

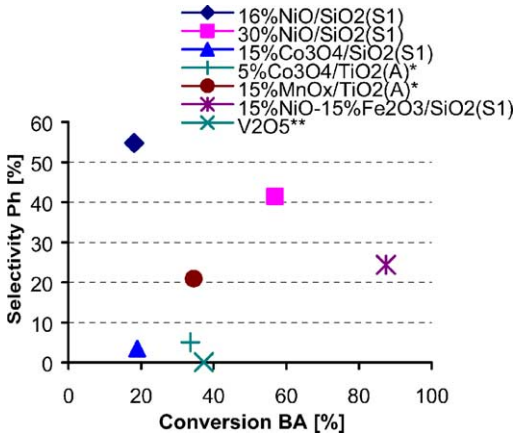

Fig. 14. Phenol selectivity vs. benzoic acid conversion over metal oxide catalysts. Reaction parameters: $T = 400\,^{\circ}C$; SV = 5.5 l g^{-1} h^{-1}; TOS ≈ 75 min. Feed composition: 1% BA, 5% O_2 (* 1.4% O_2, ** 3% O_2), 24% H_2O, balance He.

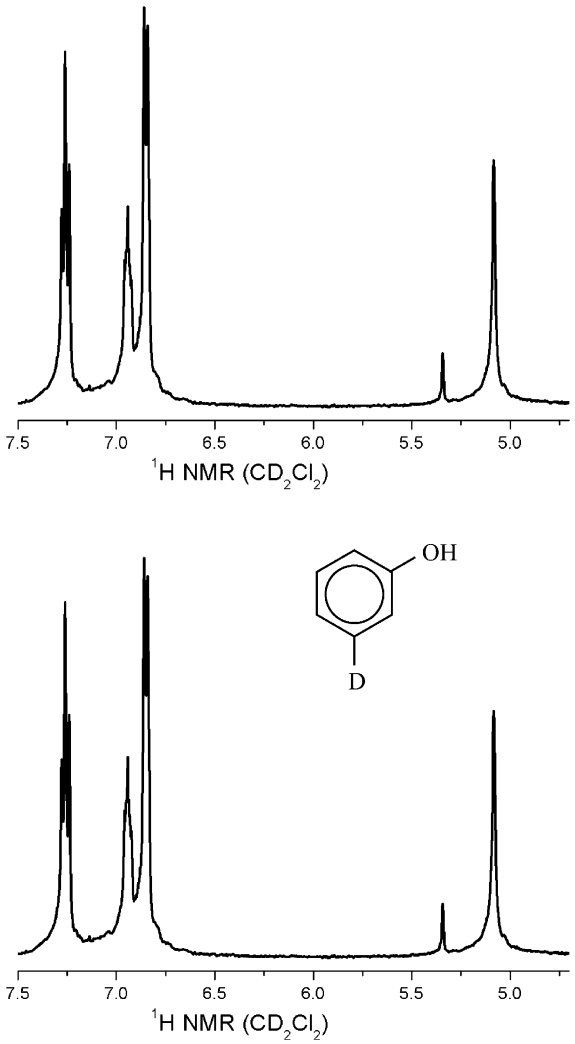

Fig. 15. ^{1}H NMR spectrum of phenol product from the gas phase oxidation of 4-D-benzoic acid (top), and ^{1}H NMR spectrum of reference 3-D-phenol (bottom).

Among the oxides tested, NiO is the most desirable for phenol production (Fig. 12). Its activity can be enhanced by addition of Fe_2O_3 modifier with minor effect on phenol selectivity, and its time-on-stream stability can be enhanced by addition of Na oxide/hydroxide. Sodium reduced the formation of coupling products possibly by eliminating the acid sites. Oxides that are known for high oxidation activities, such as V_2O_5, MnO_x and CoO_x all showed poor phenol selectivities. Instead much higher amounts of CO_x were formed.

Coupling products are formed as minor products. Of particular interest is xanthone and fluorenone. They could be formed by Friedel–Crafts acylation (Fig. 15). Biphenyl, on the other hand, is formed by coupling of decarboxylated intermediates (Fig. 16).

Regarding the reaction mechanism, two mechanisms have been suggested for copper catalysts [6–8]. In one mechanism, the reaction involves first the formation of a copper

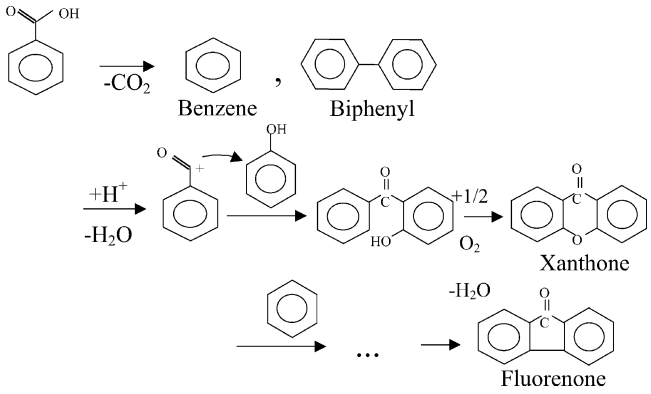

Fig. 16. Formation of by-products from benzoic acid.

dibenzoate intermediate, which is converted to a phenylbenzoate or benzoylsalicylic acid, followed by hydrolysis to phenol.

In our experiments, we could not detect any phenylbenzoate. Oxidation of *para*-D-benzoic acid resulted in exclusively *meta*-D-phenol. Thus, insertion of oxygen is in the position *ortho* to the carboxylic group. There are two possible mechanisms that could explain these results. One of them is the nucleophilic aromatic substitution of hydrogen with an oxygen ion:

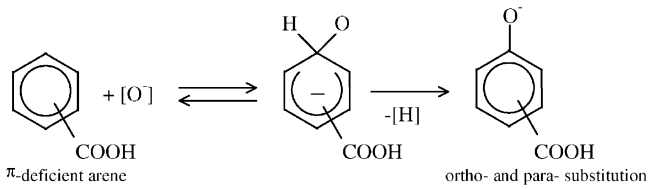

This mechanism explains the formation of a meta-deuterated product, but also suggests the formation of hydroxobenzoic acid, which was not observed in the product. A second possible mechanism involves the initial formation of a peroxoacid, followed by the transfer of an oxygen atom to the ortho position:

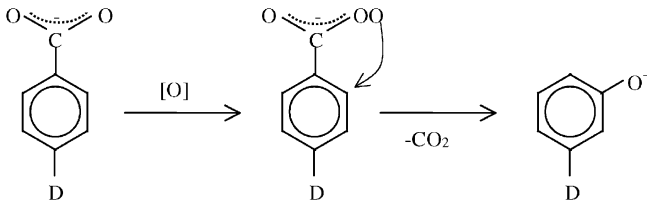

This mechanism is in good agreement with the experimental findings and is more likely applicable than the first one.

Acknowledgements

The support of this work by DOE is gratefully acknowledged.

References

[1] A.M. Thayer, Chem. Eng. News 6 (1998) 21.
[2] J. Wallace, Kirk-Othmer Encyclopedia, 4th ed., vol. 18, Wiley, New York, 1996, p. 592.
[3] J. Zhu, S.L. Andersson, J. Catal. 126 (1990) 92.
[4] D.A. Bulushev, S.I. Reshetnikov, L. Kiwi-Minsker, A. Renken, Appl. Catal. A 220 (2001) 31.
[5] B. Grzybowska-Swierkosz, Appl. Catal. A 157 (1997) 263.
[6] M. Stolkova, M. Hronec, J. Ilavsky, M. Kabesova, J. Catal. 101 (1986) 153.
[7] M. Stolkova, M. Hronec, J. Ilavsky, J. Catal. 119 (1989) 83.
[8] M. Hronec, M. Stolkova, Z. Cvengrosova, J. Kizlink, Appl. Catal. 69 (1991) 201.
[9] J. Miki, M. Asanuma, T. Konishi, Y. Tachibana, T. Shikada, A. Watanabe, US Patent 5,945,569 (1999).
[10] J. Miki, M. Asanuma, Y. Tachibana, T. Shikada, J. Chem. Soc., Chem. Commun. (1994) 691.
[11] J. Miki, M. Asanuma, Y. Tachibana, T. Shikada, J. Chem. Soc., Chem. Commun. (1994) 1685.
[12] J. Miki, M. Asanuma, Y. Tachibana, T. Shikada, J. Chem. Soc., Chem. Commun. (1994) 2679.
[13] J. Miki, M. Asanuma, Y. Tachibana, T. Shikada, Appl. Catal. A 115 (1994) L1.
[14] J. Miki, M. Asanuma, Y. Tachibana, T. Shikada, J. Catal. 151 (1995) 323.
[15] J. Miki, M. Asanuma, Y. Tachibana, T. Shikada, Appl. Catal. A 123 (1995) 111.
[16] J. Miki, M. Asanuma, Y. Tachibana, T. Shikada, Appl. Catal. A 143 (1996) 215.
[17] J. Miki, M. Asanuma, Y. Tachibana, T. Shikada, Bull. Chem. Soc. Jpn. 68 (1995) 2429.
[18] S. Ohyama, K.E. Popp, M.C. Kung, H.H. Kung, Catal. Commun. 3 (2002) 357.
[19] A.N. Shigapov, G.W. Graham, R.W. McCabe, H.K. Plummer, Appl. Catal. A 210 (2001) 287.
[20] R.D. Shoup, Colloid and Interface Science, vol. III, Academic Press, New York, 1976, p. 63.
[21] J.-Y. Yan, M.C. Kung, W.M.H. Sachtler, H.H. Kung, J. Catal. 172 (1997) 178.
[22] W.A. Dietz, J. Gas Chromatogr. 5 (1967) 68.
[23] J.D. Roberts, D.A. Semenow, H.E. Simmons Jr., L.A. Carlsmith, J. Am. Chem. Soc. 78 (1956) 601.
[24] T. Pedersen, N.W. Larsen, J. Label. Compd. 5 (2) (1969) 195.